Electronic band redistribution probed by oxygen absorption spectra of $(SrMnO_3)_n(LaMnO_3)_{2n}$ superlattices

A. Galdi,[1,*] C. Aruta,[2] P. Orgiani,[1] C. Adamo,[3] V. Bisogni,[4] N. B. Brookes,[4] G. Ghiringhelli,[5] D. G. Schlom,[3,6] P. Thakur,[4] and L. Maritato[1]

[1]*CNR SPIN - Superconductors, Oxides and Other Innovative Materials and Devices and University of Salerno, I-84084 Fisciano (SA), Italy*

[2]*CNR SPIN - Superconductors, Oxides and Other Innovative Materials and Devices and Department of Physical Sciences, I-80126 Napoli, Italy*

[3]*Department of Materials Science and Engineering, Cornell University, Ithaca, New York, 14853, USA*

[4]*European Synchrotron Radiation Facility, F-38043 Grenoble, France*

[5]*CNR SPIN - Superconductors, Oxides and Other Innovative Materials and Devices and Dipartimento di Fisica, Politecnico di Milano, I-20133 Milano, Italy*

[6]*Kavli Institute at Cornell for Nanoscale Science, Ithaca, New York 14853, USA*

(Received 6 March 2012; published 26 March 2012)

Oxygen $1s \rightarrow 2p$ (K-edge) x-ray absorption spectra mimic the density of metalliclike states of transition metal oxides, thus shedding light on the electronic band structure near Fermi energies of these compounds. We take here advantage of x-ray linear dichroism measurements at the O K edge of different $(SrMnO_3)_n(LaMnO_3)_{2n}$ superlattices, of $SrMnO_3$ and of $LaMnO_3$ thin films. X-ray linear dichroism, in the pre-edge region of the spectra, provides evidence about the specific symmetry of the Mn $3d$ orbitals hybridized with the oxygen ions, thus allowing us to disentangle the pure interface contribution from those related to strain effect and charge leakage among the superlattices' constituent blocks.

DOI: 10.1103/PhysRevB.85.125129 PACS number(s): 73.21.Cd, 71.20.−b, 75.47.Lx, 78.70.Dm

I. INTRODUCTION

The synthesis of thin film heterostructures with increasing control on interfacial roughness and composition, has nowadays made achievable the fabrication of multilayers with single-unit-cell-thick constituent blocks. Reaching such a structural limit has subsequently made it possible to create structures composed by artificial supercells, so-called superlattices (SLs), that can be considered artificial materials. In this respect, perovskite oxides combine a wide variety of functional properties with a simple structure and small lattice mismatch, so that they can be stacked on top of each other into complex multifunctional heterostructures with relative ease.[1] To study the electronic properties of both the SLs' components and the interfacial charge transfer, oxygen K-edge x-ray absorption spectroscopy (XAS) is an invaluable tool. Indeed, since the O^{2-} ion $2p$ orbitals are nominally full[2] and hybridized with the transition metal empty states, the oxygen $1s \rightarrow 2p$ transition absorption spectrum (O K edge) maps the unoccupied density of states (DOS) of predominant metal character, giving direct insights in the electronic bands' redistribution. Nevertheless, for SL systems, few XAS investigation at the oxygen edge have been reported. In this work we take advantage of O K-edge absorption spectra collected with linear polarized light to obtain important information on the competition between bulk and interface effects in different period $(SrMnO_3)_n/(LaMnO_3)_{2n}$ $[(SMO)_n/(LMO)_{2n}]$ digital SLs. Several authors reported on the fabrication, characterization, and properties of $(SMO)_n/(LMO)_{2n}$ SLs,[3–6] and consequently a number of theoretical studies have been developed to comprehend the diverse magnetic and electronic phases they exhibit.[7–9] The $(SMO)_n/(LMO)_{2n}$ SLs can be seen as a way to introduce Sr doping in LMO (La : Sr = 2 : 1) without introducing substitutional disorder.[3,4] More important, in such ordered structures, the number and the coupling of highly metallic interfaces lying at SMO/LMO interfaces can be easily tuned by changing the thickness of the constituent blocks.[10] Lattice distortions, epitaxial strain,[7,8] and orbital occupancy[9] have to be taken into account in theoretical models because of the interplay between electron and lattice and between orbital and magnetic degrees of freedom in manganite compounds.[11] X-ray linear dichroism (XLD) at the Mn L_{23} edge of $(SMO)_n/(LMO)_{2n}$ SLs has shown the preferential e_g orbitals occupation of Mn^{3+} ions.[12] The resulting orbital occupation results directly correlates to the average lattice parameter when the electronic charge is uniformly distributed in the SL (e.g., $n = 1$ sample), while, when the electrons are confined in the LMO layers, it is determined by the strain in the LMO block ($n = 5; 8$). However, because XLD spectra are dominated by the Mn^{3+} contribution,[12,13] little information can be obtained about the charge reconstruction effect on the SMO energy levels (where Mn mainly assumes $4+$ valence), and, more significantly, about the build up of electron states at the Fermi level because of the metallic interfaces. In this respect, oxygen K-edge XLD will prove to be an extremely powerful tool, not only in the specific SMO/LMO case, but more generally in the study of electronic band evolution in transition metal oxide systems and oxide heterostructures.

II. EXPERIMENT

$(SMO)_n/(LMO)_{2n}$ SLs were deposited by repeating a supercell composed by n pseudocubic unit cells of SMO and $2n$ of LMO by shuttered layer-by-layer molecular beam epitaxy (MBE).[5] For comparison, SMO and LMO thin films were also grown in the same experimental condition as the SLs. All the films were deposited on (100) $SrTiO_3$ (STO) substrates, and the overall thickness was kept fixed (23 nm for all samples except for $n = 8$, 20 nm).[5] All the investigated samples are in-plane

fully strained, so that the LMO cell is tetragonally elongated in the out-of-plane direction, while the SMO cell is compressed. The constituent blocks thus experience a modulated strain, and the SMO/LMO interfacial regions are therefore severely stressed.[12] The XAS measurements have been performed at the ID08 beamline of the European Synchrotron Radiation Facility (Grenoble, France), which is based on AppleII undulator source, allowing full control of polarization. The absorption signal has been detected by the total electron yield (TEY) technique with the incident beam at fixed grazing incidence of 30°. XLD is defined as the difference in the XAS measurement with horizontal (H, in our setting nearly ∥ to film c axis ∥ z) and vertical (V ∥ to film a-b plane ∥ xy) polarizations. XLD is sensitive to the axial anisotropy of the DOS, as V and H polarized photons mainly excite the electrons in empty states along the electric vector direction. In all the XAS measurements a constant background was fitted to the pre-edge region of the O K edge and subtracted from the spectra, which are then normalized to unity about 50 eV above the threshold. The normalized spectra are then subtracted to obtain the XLD spectrum (namely V − H).

III. RESULTS AND DISCUSSION

A. X-ray isotropic absorption spectra

In Fig. 1 we report the isotropic O K-edge XAS spectra of the $n = 1$, 5, and 8 superlattices, and of the LMO and SMO films, obtained as (V + H)/2. According to literature,[14] the region between 528 eV and 534 eV (pre-edge) is assigned to the hybridization with the Mn 3d orbitals, the peaks at about 536 eV in LMO and 538 eV in SMO are attributed to the La 5d and Sr 4d respectively, and finally the broad peak at higher energy is assigned to Mn 4sp orbitals. In particular, pre-edge region originates from the empty levels of the Mn 3d orbitals involved in the conduction and in the magnetic interactions, thus being directly correlated to the magnetotransport properties in manganites, while the states

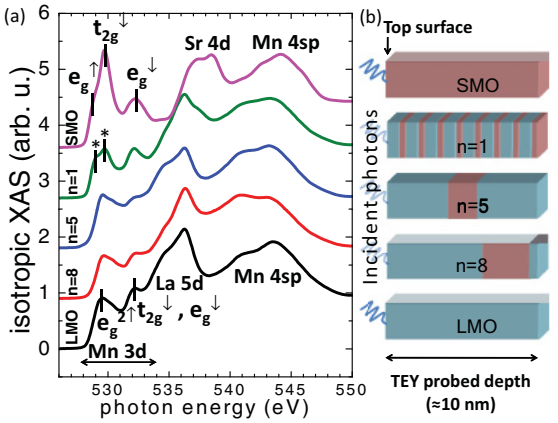

FIG. 1. (Color online) (a) Oxygen K-edge isotropic absorption spectra at 10 K, obtained as (V + H)/2, where V and H are the absorption spectra with vertical and horizontal polarization of the incident photons respectively. The spectra have been shifted vertically for clarity. (b) Sketch of the fraction of the samples probed by TEY (≈ 10 nm from top surface). As the SLs are grown starting by the SMO layer (pink),[5] LMO (blue) is always on top.

above 534 eV of predominant La/Sr character are not relevant in this sense.

As clearly evident, none of the SL spectra can be interpreted as a bare superposition of LMO and SMO ones. More important, even if the LMO : SMO ratio is the same in all the SLs (i.e., La : Sr = 2 : 1), the different periodicity (i.e., the number of conducting interfaces decreases with n) originates different features, as a consequence of the different distribution of the charge density[12] and of the nucleation of the ferromagnetic metallic phase at the interfaces.[6,15] The pre-edge features of the LMO and SMO samples are correlated to the hybridization with the bands originating from the Mn 3d levels, which are split into two spin states (up ↑ and down ↓, respectively) by the on-site exchange interaction and into e_g and t_{2g} states by the oxygen octahedron cubic crystal field. The features in the SMO spectrum can be identified with the Mn 3d character bands obtained in the LDA + U calculations,[16] that predict the splitting of $e_g^{\uparrow}$ and $t_{2g}^{\downarrow}$ levels, easily recognizable near the absorption threshold in Fig. 1. According to literature,[17–19] we label $e_g^{\uparrow}$ the peak at about 529 eV, $t_{2g}^{\downarrow}$ between 529.5 eV and 530 eV and $e_g^{\downarrow}$ close to 532 eV.

Differently from the SMO case, the electronic structure in LMO is still debated. Despite many theoretical and experimental works, several authors reported different indexing of the features of the pre-edge of LMO (or other Mn^{3+} manganites),[17,18] In case of the LMO, Mn^{3+} ions are Jahn-Teller active, so that the e_g levels split as a consequence of the distortion of the oxygen octahedron in an occupied $e_g^{1\uparrow}$ and empty $e_g^{2\uparrow}$.[20] Because of the strain-stabilized distortion in LMO thin films on STO, oxygen octahedrons are tetragonally elongated, as also demonstrated by XLD at the Mn L edge reported in Ref. 12. As a consequence, the low-energy $e_g^{1\uparrow}$ orbital has $3z^2$-r^2 symmetry, while the high-energy $e_g^{2\uparrow}$ orbital has x^2-y^2 symmetry. Accordingly, the prepeak feature just below 530 eV is then attributed to the $e_g^{2\uparrow}$ band with x^2-y^2 symmetry, while the feature at about 532 eV is attributed to a mixing of the minority bands with e_g and t_{2g} character. The superposition of the $e_g^{\downarrow}$ and $t_{2g}^{\downarrow}$ bands is also predicted in the LDA + U calculations[16] and it is determined by the electron correlations. Those results are fully consistent with the LMO band structure obtained by cluster model analyses of photoemission and O K-edge XAS spectra,[21] and by the results of optical conductivity measurements.[19]

The $(SMO)_1/(LMO)_2$ SL isotropic XAS spectrum is similar to the one of the $La_{2/3}Sr_{1/3}MnO_3$ (LSMO) alloy[22] (i.e., where La and Sr are randomly distributed within the compound). Such a result is directly correlated to the electrical charge density, which is expected to be homogeneous in this sample and equal to 0.33 holes per Mn ion. Furthermore, a double peak structure [evidenced by the asterisks in Fig. 1(a)] at about 528.5 eV and 529.5 eV can be distinguished. Such a structure is typical of the ferromagnetic metallic state.[17] As a matter of fact, in our case the $n = 1$ SL is metallic at any investigated temperature and its Curie temperature is $T_C \approx 350$ K.[10] Despite the transport,[10] magnetic,[5,6] and orbital occupation[12] properties observed in the $n = 1$ SL are also similar to those observed in LSMO thin film under tensile strain on STO,[22] the presence of the ordered metallic interfaces

originates a different electronic structure in the vicinity of the Fermi level, as shown in the following.

B. X-ray linear dichroism spectra

The empty oxygen $2p$ states inherit the axial anisotropy of the transition metal states they are hybridized with, giving rise to a measurable XLD signal, and allowing to explore the symmetry of the empty DOS.

XLD spectra of all SLs, together with the spectrum of a LSMO alloy sample, (measurement from Ref. 22) are reported in Fig. 2. The O K-edge XLD of the alloy and the $n = 1$ sample shows substantial differences which are not revealed neither in the isotropic or in the Mn $L_{2,3}$ edge spectrum. In particular, a nearly opposite behavior is found at the absorption threshold between 528 eV and 530 eV (i.e., the region attributed[22] to the hybridization with the $e_g^{\uparrow}$ electrons close to the Fermi level). The behavior of the alloy sample was explained[22] in terms of intrinsic width of the Mn states projected onto the O $2p$ larger than the tetragonal distortion crystal field (see the sketch in Fig. 2). However, for the $n = 1$ SL, the observed XLD behavior is consistent with a simple model based on different intrinsic width for the two Mn $e_g^{\uparrow}$ states. More in detail, the more occupied $e_g^1 : x^2\text{-}y^2$ level is larger than the $e_g^2 : 3z^2\text{-}r^2$ one, as depicted in Fig. 2. Bandwidth modifications and shifts of the energy of the e_g levels at the manganite interfaces have been already predicted.[23,24] It was demonstrated that the effective hopping parameter is reduced for the band originating from orbitals crossing the interface (namely the $3z^2\text{-}r^2$ orbital). Moreover, the $x^2\text{-}y^2$ and $3z^2\text{-}r^2$ energy levels are shifted a different amount depending on the nature of the interface (e.g., metallic, insulating), leading to a different orbital occupation. In SLs the electrons in $3z^2\text{-}r^2$ orbitals experience a potential energy barrier going from the LMO to the SMO side.[7] The bandwidth of the $3z^2\text{-}r^2$ electrons is therefore expected to be reduced at the interfaces with respect to the one of the $x^2\text{-}y^2$. In the $n = 1$ SL, because of the high interface density (2/3 of the Mn ions lie at the LMO/SMO interface), such a phenomenon

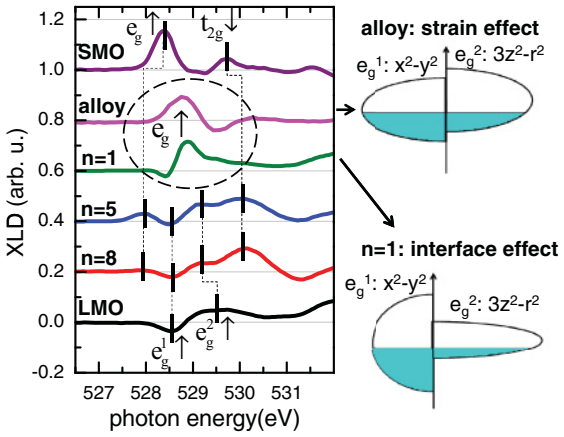

FIG. 2. (Color online) XLD spectra at 10 K of all the analyzed samples and of a LSMO sample, indicated as alloy (measurement from Ref. 22). The spectra have been shifted vertically for clarity. On the right we present a simplified drawing of the Mn-O hybridized states close to the Fermi level for the alloy and the $n = 1$ SL samples.

dominates any others. Moreover, it occurs despite the weak potential modulation, which allows the e_g electrons to be uniformly distributed within the whole SL.[7] The different energy shift favors the $3z^2\text{-}r^2$ occupation in case of a vacuum interface,[23] but $x^2\text{-}y^2$ preferential occupation can be indeed obtained in case of different interfaces.[24] Moreover, calculations indicate that in this specific case, antiferromagnetic (AF) order is then established at the interface. Indeed, in the $n = 1$ SL the occurrence of an in-plane easy axis AF component was unambiguously observed.[12]

The $n = 5$ and 8 SLs are composed by thick blocks of LMO (10, 16 unit cells, respectively) and SMO (5, 8 unit cells). Differently from the $n = 1$ SL, the charge density in these samples is not homogeneous.[6,7,12] In more detail, Mn ions in the inner part of LMO blocks assume an electronic valence close to $3+$ while assuming a valence close to $4+$ within the SMO blocks.

We start by discussing the XLD of SMO and LMO films, reported in Fig. 2. The positive feature at the edge rise of SMO XLD spectra clearly shows that unoccupied bands just above the Fermi energy have in-plane holes symmetry, according to the splitting of the energy levels induced by the tensile strain, that pushes the $3z^2\text{-}r^2$ orbital to higher energy than the $x^2\text{-}y^2$ one. The XLD intensity steeply decreases at higher energy (especially if compared to the XAS intensity) because the bandwidth of the Mn $3d$ levels projected on the oxygen states is larger than their splitting, leading to a mixing of states of different symmetry. Conversely in the LMO XLD spectrum, a negative feature at about 528.5 eV indicates the presence of holes in the $e_g^{1\uparrow}$ level with $3z^2\text{-}r^2$ symmetry, that is expected to be fully occupied. Such a feature originates from small oxygen stoichiometry variations[18,25,26] that affect the hole content in LMO, turning the sample into an insulating and weakly ferromagnetic state,[5] typical of doped LMO for hole content $x \lesssim 0.16$. Finally, a positive feature at 529.5 eV corresponds to the empty $e_g^{2\uparrow}$ with $x^2\text{-}y^2$ symmetry.

The $n = 5,8$ XLD is closer to the one observed on LMO, even though additional features appear. In particular, a double peak between 529 eV and 530 eV, and a positive one just below the absorption threshold (528 eV) (even if very weak in the $n = 8$ SL) were observed. These features cannot originate from the interface, being absent in the $n = 1$ sample, which can be considered an all-interface sample. The feature at 530 eV, is more intense in the $n = 8$ sample. Such an occurrence is related to the finite probing depth of the TEY technique [see Fig. 1(b)]. In fact, a larger fraction of LMO (therefore consequently a smaller fraction of SMO) is probed in the $n = 5$ SL (LMO : SMO = 4 : 1) with respect to the $n = 8$ SL.[12] As more SMO is probed in $n = 8$ SL sample (while we probe the same number of interfaces, namely 3), we attribute the feature to the SMO $t_{2g}^{\downarrow}$ contribution, nevertheless it appears at lower energy (between 529.5 eV and 530 eV) in the SMO single layer. As a matter of fact, in the SL samples, two factors should be taken into account to explain the shift of the SMO features. The first one is structural: in the SLs, LMO and SMO blocks experience a modulated strain, while the LMO and SMO single layers, though deposited in the same conditions, partially relax the epitaxial strain induced by the substrate along their thickness. The second one is related to charge redistribution:

electrons leak from the LMO blocks into the SMO ones, so that the SMO in SLs is indeed lightly doped.[7,12] The feature at 528 eV, more intense in the $n = 5$ sample, indicates the presence of empty states with in plane symmetry, and can be correlated to the SMO $e_g^{\uparrow}$ feature. As it is more evident in the $n = 5$ SL, though we probe less SMO, such a feature is shifted to lower energy, thus becoming more visible, as a consequence of the higher electron doping in the SMO block in this sample [see Fig. 3(a)]. On the contrary, the negative feature at 528.5 eV is associated to doped holes in the LMO block (with $3z^2$-r^2 symmetry), that are provided by interface doping and eventually by local defects (as in the pure LMO films).

IV. CONCLUSION

We can now review all the collected results within a consistent scenario of the electronic bands for the LMO, SMO and $n = 1$ SL (Fig. 3).

Our findings on the SMO and LMO are in full agreement with the results of LDA + U calculations,[16] by considering in addition the strain induced splitting of t_{2g} and e_g levels in SMO and the presence of an impurity level in LMO. Nanda and Satpathy,[7] showed that in SLs bulklike behavior is already recovered in the SMO block in the MnO_2 layer next to the interface, while it is recovered further away within the LMO block (namely, two layers). Accordingly, in large-period SLs ($n = 5,8$), the interface contribution to isotropic and XLD spectra is negligible, while the contribution of the LMO and SMO blocks modified by the strain and by the charge leakage is clearly observed. In the $n = 1$ SL, the interface density is so high that the interface induced band modifications dominate and determine the XLD behavior. The band structure we sketch in Fig. 3(c) is in agreement with the one calculated by Nanda and Satpathy[7] for the $n = 1$ SL by the GGA+U approximation, though in their work the effect of interfaces on the bandwidth of the $e_g^{\uparrow}$ levels is not evidenced.

By means of XLD measurements at the O K edge we were able to study the metal bands hybridized with the oxygen of a series of SL samples with different periodicity. Furthermore, pure SMO and LMO samples were investigated and compared to previous results obtained on alloyed LSMO samples.[22] The analysis of the isotropic and XLD spectra demonstrates that a band model based on LDA + U calculations for the SMO and LMO samples successfully describes all the observed phenomena. In the case of $n = 1$ SL and alloyed LSMO films, despite the homogeneous carrier density along their thickness and a similar average lattice parameter, XLD spectra reveals

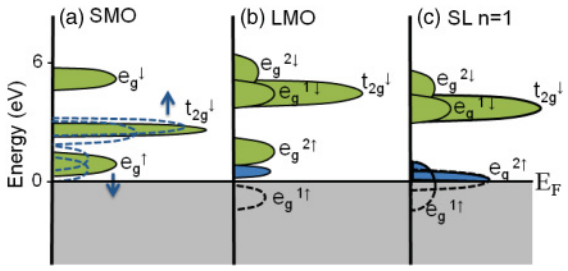

FIG. 3. (Color online) Sketch of the one-electron DOS projected on the Mn states of (a) SMO, (b) LMO, (c) $n = 1$ SL; the grey region below E_F represents the occupied DOS that cannot be directly probed by XAS. Green color indicates the features already reported in the results of Ref. 16, blue indicates the additional features provided by XLD analysis. In particular: in (a) the splitting of the e_g and t_{2g} orbitals by the strain distorted crystal field (dashed lines) and the shift of the e_g and t_{2g} levels envisaged in the lightly doped SMO in SLs (arrows); in (b) some states of $e_g^{\downarrow}$ symmetry just above the Fermi level, originating from Mn^{4+} impurities; in (c) the different bandwidth of the $e_g^{\uparrow}$ levels.

profound differences between the two cases. In particular, a modulated electrostatic potential at the LMO/SMO interfaces determines the energy width of the $e_g^{\uparrow}$ bands, which are involved in the conduction phenomena. However, for the $n = 5$ and 8 samples, in which highly metallic interfaces are more diluted within the structures, XLD analysis shows that the charge leakage at the interfaces leads to a modification of the electronic bands of the LMO and SMO constituent blocks. From our experimental results, we were able to identify the features induced by the presence of the highly conductive interfaces and their relative weight with respect to the bulklike block contribution. The O K-edge XAS, being a probe of the unoccupied DOS, allows testing of the validity of band calculations in a very straightforward way, and it is then a powerful tool in the analysis of complex nanostructured systems, where the applicability of models mainly conceived for bulk systems is not a trivial issue.

ACKNOWLEDGMENTS

This work was supported by the Italian Ministry of Education, Universities and Research (MIUR), Grant No. PRIN 20094W2LAY, "Ordine orbitale e di spin nelle eterostrutture di cuprati e manganiti". C.A. and D.G.S. acknowledge the support of the National Science Foundation MRSEC program through DMR-1120296.

*agaldi@unisa.it

[1] P. Zubko, S. Gariglio, M. Gabay, P. Ghosez, J.-M. Triscone, Annu. Rev. Condens. Matter Phys. **2**, 141 (2011) and references therein.
[2] M. Grioni, M. T. Czyzyk, F. M. F. de Groot, J. C. Fuggle, and B. E. Watts, Phys. Rev. **39**, 4886 (1989).
[3] A. Bhattacharya, X. Zhai, M. Warusawithana, J. N. Eckstein, S. D. Bader, Appl. Phys. Lett. **90**, 222503 (2007).
[4] A. Perucchi, L. Baldassarre, A. Nucara *et al.*, Nano Lett. **10**, 4819 (2010).
[5] C. Adamo, X. Ke, P. Schiffer *et al.*, Appl. Phys. Lett. **92**, 112508 (2008).
[6] A. Bhattacharya, S. J. May, S. G. E. te Velthuis, M. Warusawithana, X. Zhai, B. Jiang, J. M. Zuo, M. R. Fitzsimmons, S. D. Bader, and J. N. Eckstein, Phys. Rev. Lett. **100**, 257203 (2008).
[7] B. R. K. Nanda and S. Satpathy, Phys. Rev. B **79**, 054428 (2009).
[8] A. Iorio, C. A. Perroni, V. Marigliano Ramaglia, V. Cataudella, Phys. Rev. B **83**, 085107 (2011).

[9]S. Dong, R. Yu, S. Yunoki, G. Alvarez, J.-M. Liu, and E. Dagotto, Phys. Rev. B **78**, 201102(R) (2008).
[10]C. Adamo, C. A. Perroni, V. Cataudella, G. DeFilippis, P. Orgiani, and L. Maritato, Phys. Rev. B **79**, 045125 (2009).
[11]R. Maezono, S. Ishihara, and N. Nagaosa, Phys. Rev. B **58**, 11583 (1998).
[12]C. Aruta, C. Adamo, A. Galdi *et al.*, Phys. Rev. B **80**, 140405 (2009).
[13]A. Galdi, C. Aruta, P. Orgiani, N. B. Brookes, G. Ghiringhelli, M. MorettiSala, R. V. K. Mangalam, W. Prellier, U. Luders, and L. Maritato, Phys. Rev. B **83**, 064418 (2011).
[14]M. Abbate, F. M. F. de Groot, J. C. Fuggle *et al.*, Phys. Rev. B **46**, 4511 (1992).
[15]S. Smadici, P. Abbamonte, A. Bhattacharya, X. Zhai, B. Jiang, A. Rusydi, J. N. Eckstein, S. D. Bader, and J. M. Zuo, Phys. Rev. Lett. **99**, 196404 (2007).
[16]S. Satpathy, Z. S. Popović, and F. R. Vukajlović, Phys. Rev. Lett. **76**, 960 (1996).
[17]O. Toulemonde, F. Millange, F. Studer *et al.*, J. Phys.: Condens. Matter **11**, 109 (1999).
[18]J. H. Park, C. T. Chen, S. W. Cheong, W. Bao, G. Meigs, V. Chakarian, and Y. U. Idzerda, Phys. Rev. Lett. **76**, 4215 (1996).
[19]J. H. Jung, K. H. Kim, D. J. Eom, T. W. Noh, E. J. Choi, J. Yu, Y. S. Kwon, and Y. Chung, Phys. Rev. B **55**, 15489 (1997).
[20]D. Khomskii, Lect. Notes Phys. **569**, 89 (2001).
[21]T. Saitoh, A. E. Bocquet, T. Mizokawa, H. Namatame, A. Fujimori, M. Abbate, Y. Takeda, and M. Takano, Phys. Rev. B **51**, 13942 (1995).
[22]C. Aruta, G. Ghiringhelli, A. Tebano, N. G. Boggio, N. B. Brookes, P. G. Medaglia, and G. Balestrino, Phys. Rev. B **73**, 235121 (2006).
[23]M. J. Calderón, L. Brey, and F. Guinea, Phys. Rev. B **60**, 6698 (1999).
[24]H. Zenia, G. A. Gehring, G. Banach, and W. M. Temmerman, Phys. Rev. B **71**, 024416 (2005).
[25]M. Wołcyrz, R. Horyn, F. Bourée, and E. Bukowska, J. Alloys Compd. **353**, 170 (2003).
[26]P. Orgiani, C. Aruta, R. Ciancio, A. Galdi, and L. Maritato, Appl. Phys. Lett. **95**, 013510 (2009).